UC Irvine
UC Irvine Previously Published Works

Title
Fiber delivered probe for efficient CARS imaging of tissues

Permalink
https://escholarship.org/uc/item/5966s07v

Journal
Optics Express, 18(3)

ISSN
1094-4087

Authors
Balu, Mihaela
Liu, Gangjun
Chen, Zhongping
et al.

Publication Date
2010-01-21

DOI
10.1364/OE.18.002380

Copyright Information
This work is made available under the terms of a Creative Commons Attribution License, availalbe at https://creativecommons.org/licenses/by/4.0/

Peer reviewed

eScholarship.org Powered by the California Digital Library
University of California

Fiber delivered probe for efficient CARS imaging of tissues

Mihaela Balu*[1], Gangjun Liu*[1], Zhongping Chen[1,2], Bruce J. Tromberg[1,2], and Eric O. Potma[1,3]

[1]*Laser Microbeam and Medical Program (LAMMP), Beckman Laser Institute and Medical Clinic, 1002 Health Sciences Road East, University of California, Irvine, 92612*
[2] *Department of Biomedical Engineering, University of California, Irvine, 92697*
[3] *Department of Chemistry, University of California, Irvine, 92697*
∗ *Contributed equally to this work*
z2chen@uci.edu; epotma@uci.edu

Abstract: We demonstrate a fiber-based probe for maximum collection of the coherent anti-Stokes Raman scattering (CARS) signal in biological tissues. We discuss the design challenges including capturing the back-scattered forward generated CARS signal in the sample and the effects of fiber nonlinearities on the propagating pulses. Three different single mode fibers (fused silica fiber, photonic crystal fiber and double-clad photonic crystal fiber) were tested for the probe design. We investigated self-phase modulation, stimulated Raman scattering (SRS) and four-wave-mixing (FWM) generation in the fiber: nonlinear processes expected to occur in a two-beam excitation based probe. While SPM and SRS induced spectral broadening was negligible, a strong non phase-matched FWM contribution was found to be present in all the tested fibers for excitation conditions relevant to CARS microscopy of tissues. To spectrally suppress this strong contribution, the probe design incorporates separate fibers for excitation light delivery and for signal detection, in combination with dichroic optics. CARS images of the samples were recorded by collecting the back-scattered forward generated CARS signal in the sample through a multi-mode fiber. Different biological tissues were imaged *ex vivo* in order to assess the performance of our fiber-delivered probe for CARS imaging, a tool which we consider an important advance towards label-free, in vivo probing of superficial tissues.

© 2010 Optical Society of America

OCIS codes: (170.3880) Medical and biological imaging; (180.4315) Nonlinear microscopy; (190.4380) Nonlinear optics, four-wave mixing

References and links

1. J. X. Cheng, "Coherent anti-Stokes Raman scattering microscopy," Appl. Spectrosc. **91**, 197-208 (2007).
2. C. L. Evans and X. S. Xie, "Coherent anti-Stokes Raman scattering microscopy: chemical imaging for biology and medicine," Annu. Rev. Anal. Chem. **1**, 883-909 (2008).
3. F. Henry, D. Côté, M. A. Randolph, E. A. Z. Rust, R. W. Redmond, I. E. Kochevar, C. P. Lin, and J. M. Winograd, "Real-time in vivo assessment of the nerve microenvironment with coherent anti-Stokes Raman scattering microscopy," Plastic and Reconstructive Surgery **123**, 123S-130S (2009).
4. T. B. Huff, Y. Shi, Y. Yan, H. Wang, and J. X. Cheng, "Multimodel nonlinear optical microscopy and applications to central nervous system," IEEE J. Sel. Topics. Quant. Electron. **14**, 4-9 (2008).
5. T. T. Le, C. W. Rehrer, T. B. Huff, M. B. Nichols, I. G. Camarillo, and J. X. Cheng, "Nonlinear optical imaging to evaluate the impact of obesity on mammary gland and tumor stroma," Mol. Imaging **6**, 205-211 (2007).

#121040 - $15.00 USD Received 7 Dec 2009; revised 18 Jan 2010; accepted 19 Jan 2010; published 21 Jan 2010

6. H. W. Wang, I. M. Langohr, M. Sturek, and J. X. Cheng, "Imaging and quantitative ananlysis of atherosclerotic lesions by CARS-based multimoddal nonlinear optical microscopy," Artherioscler. Thromb. Vasc. Biol. **29**, 1342-1342 (2009).
7. M. Zimmerley, R. A. McClure, B. Choi, and E. O. Potma, "Following dimethyl sulfoxide skin optical clearing with quantitative nonlinear mulimodal microscopy," Appl. Opt. **48**, D79-D87 (2009).
8. C. L. Evans, E. O. Potma, M. Puoris'haag, D. Cote, C. Lin, and X. S. Xie, "Chemical imaging of tissue in vivo with video-rate coherent anti-Stokes Raman scattering (CARS) microscopy," Proc. Natl. Acad. Sci. USA **102**, 16807-16812 (2005).
9. W. Jung, S. Tang, D. T. McCormic, T. Xie, Y. C. Ahn, I. V. Tomov, T. B. Krasieva, B. J. Tromberg, and Z. Chen, "Miniaturized probe based on microelectromechanical system mirror for multiphoton microscopy," Opt. Lett. **33**, 1324-1326 (2008).
10. G. Liu, T. Xie, I. V. Tomov, J. Su, L. Yu, J. Zhang, B. J. Tromberg, and Z. Chen, "Rotational multiphoton endoscopy with a 1 μm fiber laser system," Opt. Lett. **34**, 2249-2252 (2009).
11. C. J. Engelbrecht, R. S. Johnston, E. J. Seibel, and F. Helmchen, "Ultra-compact fiber-optic two-photon microscope for functional fluorescence imaging in vivo," Opt. Express **16**, 5556-5564 (2008).
12. R. LeHarzic, I. Riemann, M. Wienigel, K. König, and B. Messerschmidt, "Rigid and high-numerical-aperture two-photon fluorescence endoscope,"Appl. Opt. **48**, 3396-3400 (2009).
13. W. Piyawattanametha, E.D. Cocker, L.D. Burns, R.P. Barretto, J.C. Jung, H. Ra, O. Solgaard, M.J. Schnitzer, "In vivo brain imaging using a portable 2.9 g two-photon microscope based on a microelectromechanical systems scanning mirror," Opt Lett. **34**, 2309-2311 (2009).
14. F. Légaré, C. L. Evans, F. Ganikhanov, and X. S. Xie, "Towards CARS endoscopy," Opt. Express **14**, 4427-4432 (2006).
15. H. Wang, T. B. Huff, and J. X. Cheng, "Coherent anti-Stokes Raman scattering imaging with a laser source delivered by a photonic crystal fiber," Opt. Lett. **31**, 1417-1419 (2006).
16. Q. T. Nguyen, P. S. Tsai, and D. Kleinfeld, "MPScope: a versatile software suite for multiphoton microscopy," J. Neurosci. Methods **156**, 351-359 (2006).
17. E. R. Andresen, S. R. Keiding, and E. O. Potma, "Picosecond anti-Stokes generation in a photonic-crystal fiber for interferometric CARS microscopy," Opt. Express **14**, 7246-7251 (2006).
18. D. G. Ouzounov, K. D. Moll, M. A. Foster, W. R. Zipfel, W. W. Webb, and A. L. Gaeta, "Delivery of nanojoule femtosecond pulses through large-core microstructured fibers," Opt. Lett. **27**, 1513-1515 (2002).
19. W. Göbel, A. Nimmerjahn, and F. Helmchen, "Distortion-free delivery of nanojoule femtosecond pulses from a To:sapphire laser through a hollow-core photonic crystal fiber " Opt. Lett. **29**, 1285-1287 (2004).
20. L. Fu, X. Gan, and M. Gu, "Nonlinear optical microscopy based on double-clad photonic crystal fibers," Opt. Express **13**, 5528-5534 (2008).
21. D. Kim, H. Choi, S. Yazdanfar, and P. T. C. So, "Ultrafast optical pulse delivery with fibers for nonlinear mircoscopy," Microsc. Res. Tech. **71**, 887-896 (2008).
22. S. Y. Ryu, H. Y. Choi, J. Na, W. J. Choi, and B. H. Lee, "Lensed fiber probes designed as an alternative to bulk probes in optical coherence tomography," Appl. Opt. **47**, 1510-1517 (2008).
23. A. Uchida, M. Takeoka, T. Nakata, and F. Kannari, "Wide-range all-optical wavelength conversion using dual-wavelength-pumped fiber Raman converter," J. Lightwave Technol. **16**, 92-99 (1998).
24. C. Xiong, Z. Chen, and W. J. Wadsworth, "Dual-wavelength-pumped supercontinuum generation in an all-fiber device," J. Lightwave Technol. **27**, 1638-1643 (2009).
25. A. Mussot, T. Sylvestre, L. Provino, and H. Maillotte, "Generation of a broadband single-mode supercontinuum in a conventional dispersion-shifted fiber by used of a subnanosecond microchip laser.," Opt. Lett. **28**, 1820-1822 (2003).
26. W. Piyawattanametha, R. P. J. Barretto, T. H. Ko, B. A. Flusberg, E. D. Cocker, H. J. Ra, D. S. Lee, O. Solgaard, and M. J. Schnitzer, "Fast-scanning two-photon fluorescence imaging system based on a microelectromechanical systems two-dimensional scanning mirror," Opt. Lett. **31**, 2018-2020 (2006).
27. L. Fu, A. Jain, H. Xie, C. Cranfield, and M. Gu, "Nonlinear optical endoscopy based on a double-clad photonic crystal fiber and a MEMS mirror," Opt. Express **14**, 1027-1032 (2006).

1. Introduction

CARS microscopy enables label-free imaging of various important bio-molecules at sub-micron resolution and at fast image acquisition rates.[1, 2] In particular, CARS imaging has made it possible to rapidly visualize lipids in tissues in vitro and in vivo. Using the high lipid sensitivity of the CARS microscope, various lipid-related diseases and lipid abnormalities can now be studied at the cellular level in intact tissues. For instance, CARS microscopy has been instrumental in providing insight into myelin degradation in the nervous system[3, 4] and in illuminating the role of lipid in mammary tumorigenesis[5] and atherosclerosis.[6] The CARS

#121040 - $15.00 USD Received 7 Dec 2009; revised 18 Jan 2010; accepted 19 Jan 2010; published 21 Jan 2010
(C) 2010 OSA

imaging properties are particularly well suited to examine superficial tissues such as skin, as demonstrated by imaging studies on human skin *ex vivo*[7] and on mouse models *in vivo*.[8] Combined with other nonlinear imaging modalities such as two-photon excited fluorescence (TPEF) and second harmonic generation (SHG), CARS contrast has proven to be a powerful diagnostic in label-free multimodal microscopy. Whereas the diagnostic capabilities of CARS microscopy are promising, the practical implementation of the technique for clinical studies is currently rather limited. A typical CARS microscope is based on laser sources with a large footprint and a dedicated research microscope, which provides limited access for *in vivo* imaging studies of human subjects. An important step in optimizing this imaging technology for clinical studies is the development of a fiber-delivered probe, which would enable patient-friendly CARS examination of superficial tissues.

Whereas significant progress has been made for handheld probes suitable for TPEF and SHG imaging[9, 10, 11, 12, 13], the development of a fiber-delivered CARS probe is currently still in its infancy. Compared to TPEF and SHG, which are induced by a single pulse train, CARS necessitates two pulse trains (pump and Stokes). Several design challenges stand out: 1) Efficient propagation of two ultrafast pulse trains of different color through an optical fiber for delivery of the excitation light at the sample, and 2) efficient collection of the backward scattered signal into the fiber for detection. An important design consideration is the suppression of optical nonlinearities in the delivery fiber, such as self phase modulation (SPM) and stimulated Raman scattering (SRS), which generally lead to unwanted spectral broadening of the pulses. In principle, the picosecond laser pulses that are often used in CARS microscopy have pulse energies that are low enough to minimize the effects of SPM and SRS. This permits the use of single mode fibers (SMF), which have been successfully used in initial designs of CARS fiber probes.[14] Compared to SMFs, the use of photonic crystal fibers (PCF) is more attractive because they can be optimized for the delivery of both picosecond and femtosecond pulse trains. PCFs are thus an excellent design choice for the development of fiber-based multimodal CARS microscopy, which incorporates TPEF and SHG modalities that often necessitate the higher pulse energy of femtosecond pulses. PCFs have been used for delivering picosecond pump and Stokes pulses to the sample[15], but successful detection of CARS signals through a PCF has yet to be demonstrated.

Maximum signal detection requires efficient coupling of the generated signal into the fiber. In CARS imaging of tissues, the strongest epi-signals originate from forward propagated, phase-matched anti-Stokes radiation that is subsequently back-scattered by the heterogeneous tissue. This implies that the captured radiation in the backward direction has lost its parfocality with respect to the focal spot of the focusing lens, which hampers coupling of the signal into the guiding core of the fiber. Using standard telecom fibers, it was found that the CARS image was affected by the selective coupling of only the parfocal epi-signal into the fiber core aperture, whereas other backward scattered CARS contributions were rejected by the fiber aperture.[14] To increase the coupling efficiency, signal can be coupled, for instance, into the cladding of a PCF. For this purpose, double-clad PCFs have been used in fiber probes suitable for SHG imaging[9], suggesting that a similar configuration can be used for the development of a CARS fiber-delivered probe.

In this work, we advance the development of a CARS fiber probe by carefully optimizing the pulse delivery and the signal collection efficiencies of the fiber. An important finding in this work is that for all the fibers tested, a strong four-wave-mixing (FWM) contribution at the anti-Stokes frequency is generated in the delivery fiber under typical CARS excitation conditions. We show that this fiber-generated FWM component forms a large background that typically overwhelms the signal generated in the sample, and severely complicates the interpretation of the image unless removed. We employ a simple scheme for removing this spurious contribution

#121040 - $15.00 USD Received 7 Dec 2009; revised 18 Jan 2010; accepted 19 Jan 2010; published 21 Jan 2010
(C) 2010 OSA

based on the use of separate fibers for delivery and detection. Using this configuration, we achieve high contrast imaging of a variety of tissue samples.

2. Materials and methods

2.1. Experimental setup

The experimental set-up is described in Figure 1. A Ti:Sapphire oscillator (Mira-900, Coherent, Inc., Los Angeles, CA), delivering 280 fs pulses at 76 MHz, tunable in the 750 -920 nm range, was used as the pump beam in the CARS process. The Stokes beam was derived from a 76 MHz mode-locked laser source (picoTrain, High-Q Lasers, Austria) which produced 7.5 ps-pulsed 1064 nm light. The bandwidth of the femtosecond pulse was $\sim$150 cm^{-1} while the bandwidth of the picosecond pulse was $\sim$2.0 cm^{-1}. The two laser sources were synchronized using an active feedback scheme (High-Q Lasers, Austria). For the experiments presented in this manuscript, the femtosecond source was tuned to 817 nm, corresponding to a wavenumber of 12240 cm^{-1}, resulting in a 2842 cm^{-1} shift between the pump and Stokes pulses, which matches the Raman shift of the CH_2 stretch in lipids. The reason for chosing a femtosecond pump beam and a picosecond probe beam is twofold. First, the femtosecond pump enables two-photon excited fluorescence and second harmonic generation in the sample at high efficiency. Although the use of femtosecond pulses reduces the spectral resolution of the CARS process, the spectral resolution is sufficient for selectively detecting lipids in tissues. Indeed, the CH-stretching vibrational range extends over more than 100 cm^{-1}, implying that the spectral resolution of the experiment can be significantly relaxed in the case CARS is used for discriminating lipids from other molecular species. Second, we have deliberately chosen to use a femtosecond and picosecond pulse pair combination to test the versatility of the fiber delivered probe. A CARS fiber delivered probe should be compatible with various multiphoton modalities based on either femtosecond or picosecond excitation pulses. The pump and Stokes beams were collinearly overlapped using a dichroic mirror (1000dcxr, Chroma).

The probe design incorporates a delivery fiber, scanning optics, an objective lens and a separate fiber for signal collection. Three different single mode fibers were tested for the laser pulse delivery: a single mode fused silica fiber (HI 780, Corning, 40 cm long, NA: 0.14, mode field diameter: $\sim$4.8 μm), a double-clad DCPCF16 photonic crystal fiber (A/S DC-165-16-PASSIVE, Crystal Fibre, 80 cm long, NA: 0.04, mode field diameter: 16 μm) and a large mode area photonic crystal fiber (LMA-20, Crystal Fibre, 50 cm long, NA: 0.04, mode field diameter: $\sim$20 μm). A 4X/0.1 NA objective lens was used for coupling the light into the fibers. The sizes of the excitation beams and their divergences were independently adjusted before the fiber for maximum coupling efficiency. We used a spectrometer (USB4000-VIS-NIR Miniature Fiber Optic Spectrometer, Ocean Optics) to monitor the output spectrum of each fiber.

After passage through the delivery fiber, the pulses were directed to a dichroic mirror (760dcxr, Chroma, T: 775-1000 nm, R: 535-745 nm). Laser beam scanning was achieved with a galvanometric scanner (Cambridge Technology), and a scan lens and tube lens were used to project the excitation light onto a 63X, 0.95NA, water-immersed Zeiss objective. The average powers at the sample corresponding to 817 nm and 1064 nm were 35 mW and 25 mW, respectively. The back-scattered CARS signal was collected by the focusing objective, separated from the excitation beams by the dichroic mirror after the fiber and directed through a 1 m long multi-mode fiber (M28L01, Thorlabs, core diameter: 400 μm, NA: 0.39) to a photomultiplier tube (R7400U-20, Hamamatsu). The scan and the data collection were controlled by MPScope software.[16] The images (512 $\times$ 512 pixels) were collected at a rate of 2 s per frame.

#121040 - $15.00 USD Received 7 Dec 2009; revised 18 Jan 2010; accepted 19 Jan 2010; published 21 Jan 2010
(C) 2010 OSA

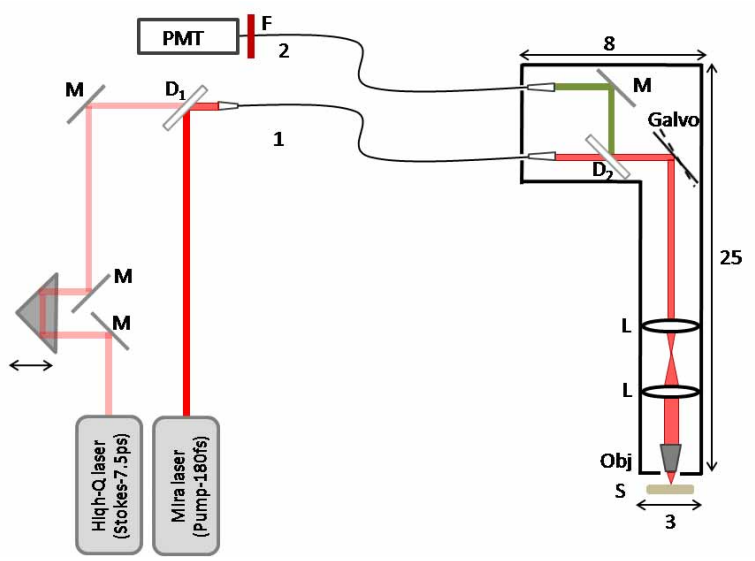

Fig. 1. Schematic diagram of the fiber-delivered probe for CARS tissue imaging: M-mirrors; D1- 1000 nm longpass dichroic mirror; D2- 760 nm longpass dichroic mirror, L-lens; Obj-objective; S-sample; F- 670 nm bandpass filter. Fiber 1 is used for delivery of the excitation pulses and fiber 2 is used for detecting the CARS radiation. The dimensions of the probe are indicated in cm.

2.2. Materials

To evaluate the performance of the handheld CARS probe, we imaged adipocytes in freshly excised samples of mouse ear (CD1/C57 black wild type mice) and rabbit skin (Pathogen-free New Zealand White rabbits Oregon Rabbit Supply). In addition, the lipid distribution in the Meibomian gland of a 2-month old mouse was examined. Eyelids from 2 month-old mice were removed and fixed in 2% paraformaldehyde in PBS. Tissue was then embedded in OCT medium, snap frozen in liquid nitrogen and sectioned to $\sim$50 μm.

3. Results and discussion

In fiber delivered SHG and TPEF microscopy, the spectral changes induced by fiber nonlinearities through SPM and SRS are often a primary concern. In CARS microscopy, which is based on the use of two pulse trains, fiber nonlinearities produce additional frequency components in addition to the spectral changes to the individual pulses. It has been shown that when pump (ω_p) and Stokes (ω_S) pulses are time-overlapped in optimized PCFs, four-wave-mixing processes can generate strong contributions at the anti-Stokes frequency ($2\omega_p - \omega_S$).[17] Depending on the phase-matching properties of the PCF, anti-Stokes components can be generated at substantial shifts up to 3000 cm^{-1}, a range of direct relevance to lipid imaging. To optimize the design of the fiber delivered probe, we first examined the effect of these fiber nonlinearities on the quality of the CARS excitation light.

Pulse delivery without significant spectral and/or temporal broadening is an important criterion for selecting a delivery fiber. Although it has been shown that pulse broadening effects are minimal in standard silica SMFs with lengths of less than 1m for picosecond pump and probe pulses with energies of a few nJ[14], such fibers do not support femtosecond pulse trains with pulse energies relevant to CARS microscopy. To avoid spectral broadening effects, PCFs have

#121040 - $15.00 USD Received 7 Dec 2009; revised 18 Jan 2010; accepted 19 Jan 2010; published 21 Jan 2010
(C) 2010 OSA

been used as the primary excitation delivery fibers in multiphoton microscopy.[18, 19]

Here we examined a double-clad photonic crystal fiber (DCPCF16, Crystal Fibre) for use in multiphoton CARS microscopy. This fiber was selected because it could potentially be used for both efficient delivery of laser light and subsequent collection of back-scattered CARS signals. Double-clad PCFs offer the possibility of collecting the back-scattered signal through the fiber cladding, while the excitation beam is delivered through the fiber core, which makes these fibers ideal for general optical imaging endoscopy applications.[20] This fiber has a 16 μm core that minimizes optical nonlinearities, which has enabled its use in endoscopic nonlinear optical imaging applications.[9, 10, 21] As expected, limited spectral broadening of both the femtosecond and picosecond pulses was observed in this fiber of length less than 1m, as depicted in Fig. 2(a).

The third fiber we tested was a large mode area PCF (LMA-20, Crystal Fibre) of 20 μm core diameter. This fiber has previously been used as a delivery and detection fiber in optical coherence tomography (OCT).[22] In this fiber, no significant spectral pulse broadening was observed, as illustrated in Figure 2b. While the temporal duration of the picosecond Stokes beam was unaffected, the fs pump increased in duration by a factor of 2.5 (from 280 fs to 700 fs).

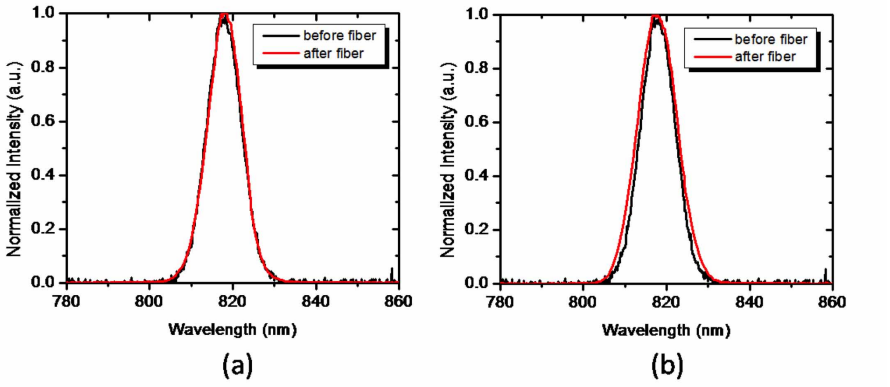

Fig. 2. Intensity spectra of the pump beam measured before and after the (a) DCPCF16 fiber (FWHM=9.7 nm before the fiber; FWHM=9.7 nm after the fiber) and (b) the LMA-20 PCF (FWHM=10 nm before the fiber; FWHM=11 nm after the fiber)

While the spectral broadening was not a concern for the individual pump and Stokes pulses in the PCF fibers, new frequency components may arise when the pump and Stokes are temporally overlapped in the fiber as a result of frequency mixing. In particular, for fibers that support phase-matching over a wide bandwidth, anti-Stokes frequency components can be generated through a FWM process in the fiber. To suppress such FWM effects, we selected PCF fibers that do not support phase-matching of the frequency components shifted by $\sim$3000 cm^{-1} relative to the zero dispersion wavelength of the fiber. Hence, our fibers fulfill the condition:

$$(2\beta_p - \beta_S + \beta_{as}) \cdot L = \Delta\beta \cdot L >> |\pi| \tag{1}$$

where β_p, β_S and β_{as} are the wave vectors of the pump, Stokes and anti-Stokes components, respectively, and L is the length of the fiber over which the frequency components remain temporally overlapped. Under these conditions, no coherent anti-Stokes generation is expected through a nonresonant FWM process. Despite the phase mismatch between the frequency com-

#121040 - $15.00 USD Received 7 Dec 2009; revised 18 Jan 2010; accepted 19 Jan 2010; published 21 Jan 2010
(C) 2010 OSA

ponents, we observed significant anti-Stokes generation in the PCF fibers. The spectral content of the anti-Stokes shifted radiation is shown in Fig. 3. The isolated anti-Stokes component shows a well-defined spectral profile that corresponds to the spectral convolution of the pump and Stokes pulse spectra. Because no additional broadening of this shifted component is observed, we conclude that this contribution is generated directly through a nonlinear mixing process between the pump and the Stokes pulses, and thus independent of the SPM mechanism. Importantly, we observed an identical anti-Stokes component in the case of the silica SMF, confirming that the anti-Stokes radiation is not the result of accidental phase-matching in the PCF fiber. We verified that the intensity of the anti-Stokes component scales quadratically with the pump light and linearly with the Stokes radiation, confirming that this shifted contribution is the result of a four-wave-mixing process.

FWM in fibers using two pump beams of different color is a well-known mechanism of generating new frequency components around the zero dispersion wavelength.[23, 24] However, such mechanisms typically rely on phase-matched conditions and the limited width of the Raman gain spectrum in silica, resulting in only moderate spectral shifts (≤ 500 cm^{-1}) relative to the input beams. Specially tailored PCFs with exceptionally broad phase-matching conditions have been used to achieve FWM generation of components shifted as much as 3000 cm^{-1}.[17] Large shifts under non-phase-matching conditions can be achieved through cascaded stimulated Raman scattering, producing an array of periodically spaced spectral components.[25] Such spectral patterns are not observed in our experiments, suggesting that stimulated Raman processes based on the fundamental Si-O modes are not the primary source of the observed anti-Stokes radiation. A possible explanation for the observed FWM component is the population of higher lying vibrational states of Si-O overtones and fiber impurities through stimulated Raman pumping, followed by incoherent anti-Stokes scattering by the pump. The incoherent anti-Stokes light is sustained in the fiber as it is not affected by phase-matching with the pump and Stokes beam.

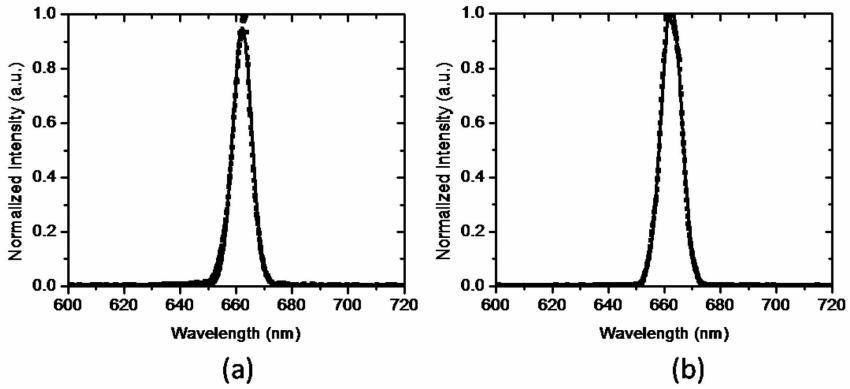

Fig. 3. Spectrally-resolved anti-Stokes four-wave-mixing signal measured at the output of (a) the LMA20 fiber (FWHM=7.9 nm) output and (b) the silica SMF (FWHM=8.6 nm).

In all fibers tested here, the anti-Stokes component generated in the fiber was much stronger than the typical CARS signals generated in biological samples. We compared the strength of the anti-Stokes FWM signal to the CARS signal generated in a DMSO sample after the fiber. The comparison between the two signals as a function of the time delay between the pump and the Stokes pulses is presented in Figure 4 for the double-clad PCF and for the LMA-20 PCF. A two meter long double-clad PCF was also used in an effort to separate the fiber anti-Stokes

#121040 - $15.00 USD Received 7 Dec 2009; revised 18 Jan 2010; accepted 19 Jan 2010; published 21 Jan 2010
(C) 2010 OSA

component from the CARS signal generated in the fiber due to a longer walk-off distance of the pump and Stokes propagating pulses. However, we found this measure to be ineffective: the FWM signal from the fiber could not be sufficiently suppressed without significantly affecting the CARS signal generated in the sample.

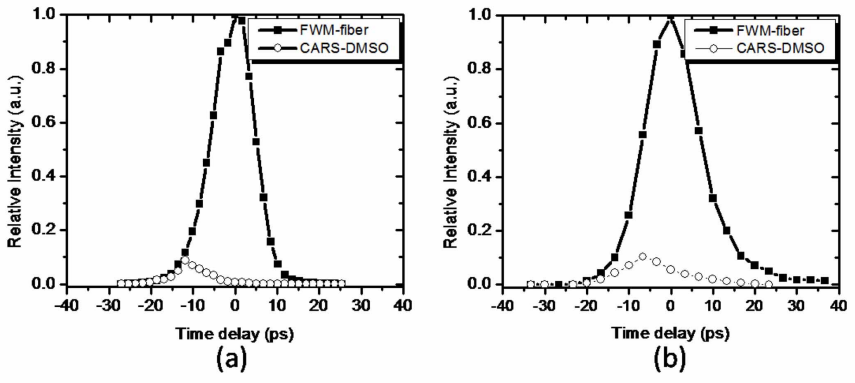

Fig. 4. CARS signal intensity from the DMSO sample and FWM from the fiber as a function of time delay between the pump and the Stokes beam for the DCPCF16 fiber (a) and the LMA-20 fiber (b).

Given the observed fiber nonlineartities, we have chosen to use a photonic crystal fiber because of its favorable dispersion properties relative to a standard single mode optical fiber. The presence of intrinsic anti-Stokes generation in the fiber necessitates spectral filtering of the excitation light before focusing it into the sample. We have, therefore, chosen to implement separate fibers for delivery of the excitation light and collection of the signal.[11, 12] We selected the large area PCF (LMA20) for laser pulse delivery because of its excellent suppression of spectral broadening effects. The 4X/0.1 NA objective used for fiber coupling provided a coupling efficiency of 40% for 817 nm and 20% for 1064 nm. Since maximum efficiency of this fiber corresponds to 780 nm, a higher coupling efficiency for 817 nm than for 1064 nm was expected. The average power after the fiber was $\sim$80 mW for both beams. The anti-Stokes radiation generated in the fiber was filtered out by a dichroic mirror placed after the fiber. The back-scattered forward generated CARS signal in the sample was collected by a second fiber. The collection fiber was chosen to be a large mode area, multi-mode fiber for maximum collection. A collection efficiency of 80% was obtained by matching the 0.39 NA of the fiber with the 0.4 NA of the objective used for fiber coupling.

To assess the performance of our fiber-delivered probe for CARS imaging, we imaged three different biological tissues ex vivo. We chose to take images of skin and eyelid, superficial tissues that would be easy to access in future in-vivo imaging. Subcutaneous fat (5(a)), individual adipocytes (Fig. 5(b)) and meibocytes (Fig. 5(c)) are clearly resolved with high contrast. The contrast observed is comparable to the contrast seen in CARS images obtained through free-space detection of the back-scattered light.[8] This suggests that the detected signal includes the back-scattered, forward generated CARS radiation, and that the contrast is not dominated by aperture effects at the detection fiber. In addition, the contrast is not affected by spurious anti-Stokes components from the delivery fiber, resulting in images that originate solely from CARS generation in the tissue.

The present images demonstrate that our design of separate delivery and detection fibers provides a simple yet efficient approach for acquiring high quality CARS images free of spectral

#121040 - $15.00 USD Received 7 Dec 2009; revised 18 Jan 2010; accepted 19 Jan 2010; published 21 Jan 2010
(C) 2010 OSA

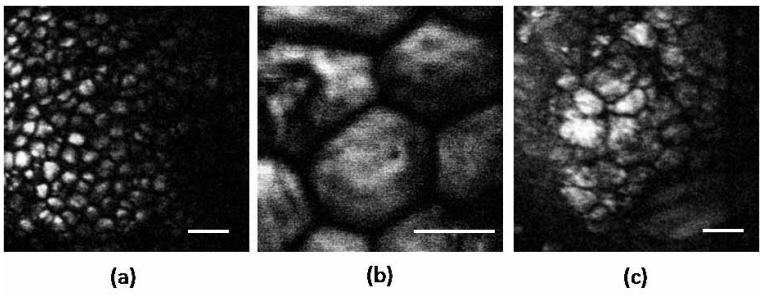

Fig. 5. CARS images of thick tissue samples *ex vivo* at 2842 cm^{-1}.a) Small adipocytes of mouse ear skin. b) Adipocytes of subcutaneous layer of rabbit skin tissue. C) Meibomian gland in mouse eyelid. Images were acquired in 2s. Scale bar is 50 μm.

artifacts and aperture effects. Although our present design produces acceptable CARS images, further miniaturization will be required to optimize its use as a hand-held probe suitable for clinical studies. Based on the current scheme, such optimization can be achieved by incorporating MEMS scanners and miniature lenses.[13, 26, 27]

4. Conclusion

We have demonstrated a fiber-delivered probe suitable for CARS imaging of thick tissues. Our design is based on two advances. First, we identified that a major problem in CARS probe design is the presence of a very strong anti-Stokes component in silica delivery fibers generated through a FWM process. Without proper spectral filtering, this component affects the CARS image from the tissue sample. Our scheme efficiently suppresses this spurious anti-Stokes component through the use of a separate fiber for excitation delivery and for signal detection, which allows the incorporation of dichroic optics for anti-Stokes rejection. Second, we optimized the detection of backscattered CARS radiation from the sample by using a large core multimode fiber in the detection channel. This scheme produces high quality CARS images free of detector aperture effects. We expect that further miniaturization of this fiber-delivered probe will result in a handheld probe for clinical CARS imaging.

Acknowledgments

This work was supported by the National Institutes of Health (NIH) (EB-00293, CA-91717, RR- 01192), National Science Foundation (NSF) (BES- 86924), Air Force Office of Scientific Research (AFOSR) (FA9550-04-0101), and the Beckman Laser Institute Endowment.

#121040 - $15.00 USD Received 7 Dec 2009; revised 18 Jan 2010; accepted 19 Jan 2010; published 21 Jan 2010
(C) 2010 OSA